Published in "Biochimica et Biophysica Acta (BBA) - Molecular Cell Research 1863(12): 2905–2915, 2016" which should be cited to refer to this work.

Endogenous TRPV1 stimulation leads to the activation of the inositol phospholipid pathway necessary for sustained Ca^{2+} oscillations

László Pecze *, Walter Blum, Thomas Henzi, Beat Schwaller

Anatomy, Department of Medicine, University of Fribourg, Route Albert-Gockel 1, Fribourg, CH-1700, Switzerland

Sensory neuron subpopulations as well as breast and prostate cancer cells express functional transient receptor potential vanilloid type 1 (TRPV1) ion channels; however little is known how TRPV1 activation leads to biological responses. Agonist-induced activation of TRPV1 resulted in specific spatiotemporal patterns of cytoplasmic Ca^{2+} signals in breast and prostate cancer-derived cells. Capsaicin (CAPS; 50 μM) evoked intracellular Ca^{2+} oscillations and/or intercellular Ca^{2+} waves in all cell lines. As evidenced in prostate cancer Du 145 cells, oscillations were largely dependent on the expression of functional TRPV1 channels in the plasma membrane, phospholipase C activation and on the presence of extracellular Ca^{2+} ions. Concomitant oscillations of the mitochondrial matrix Ca^{2+} concentration resulted in mitochondria energization evidenced by increased ATP production. CAPS-induced Ca^{2+} oscillations also occurred in a subset of sensory neurons, yet already at lower CAPS concentrations (1 μM). Stimulation of ectopically expressed TRPV1 channels in CAPS-insensitive NIH-3T3 cells didn't provoke CAPS-triggered Ca^{2+} oscillations; rather it resulted in low-magnitude, long-lasting elevations of the cytosolic Ca^{2+} concentration. This indicates that sole TRPV1 activation is not sufficient to generate Ca^{2+} oscillations. Instead the initial TRPV1-mediated signal leads to the activation of the inositol phospholipid pathway. This in turn suffices to generate a biologically relevant frequency-modulated Ca^{2+} signal.

1. Introduction

Calcium ions (Ca^{2+}), universal signaling molecules, are widely recognized to play a fundamental role in the regulation of various biological processes. Many cytosolic and mitochondrial activities are driven in a Ca^{2+}-dependent manner. Therefore, each cell possesses sophisticated mechanisms for the precise regulation of cytoplasmic (c_{cyt}), endoplasmic reticulum luminal (c_{ER}) and mitochondrial matrix (c_{mito}) Ca^{2+} concentrations. Since Ca^{2+} regulates the cell cycle at several stages, Ca^{2+} signaling is importantly involved in cell-fate determination (quiescent state, proliferation or cell death). Mitogenic compounds such as platelet-derived growth factor, vasopressin, prostaglandin, bombesin or EGF evoke repetitive Ca^{2+} transients and also induce inositol trisphosphate ($InsP_3$) production [1,2]. In Swiss 3T3 cells, increases in c_{cyt} evoked by mitogenic compounds are essential, but not sufficient to induce DNA synthesis and proliferation [3]. Moreover the frequency of base-line spiking Ca^{2+} oscillations in cultured human embryonic kidney (HEK) cells is directly related to cell proliferation [4]. In postmitotic neurons, Ca^{2+} oscillations regulate a variety of neuronal processes including excitability, associativity, neurotransmitter release, synaptic plasticity and gene transcription [5].

The signaling process leading to Ca^{2+} oscillations is composed of the following steps: I) A ligand binds to its receptor coupled to heterotrimeric G proteins, II) the $G_{\alpha q}$ subunit of a heterotrimeric G protein dissociates from the G protein-receptor complex and activates phospholipase C, III) phospholipase C hydrolyzes phosphatidylinositol 4,5-bisphosphate (PIP2) to inositol 1,4,5-trisphosphate ($InsP_3$), which then releases Ca^{2+} from intracellular stores via binding to the inositol trisphosphate receptor ($InsP_3R$) [6] and diacylglycerol (DAG), which activates protein kinase C (PKC) and IV) activation of $InsP_3R$ by $InsP_3$ leads to the quantal release of Ca^{2+} ions from the endoplasmic reticulum [7]. The shape of the Ca^{2+} signal is correlated with the $InsP_3$ concentration, i.e. the stimulation intensity: weak activation results in single Ca^{2+} spikes, increasing the stimulation leads to slow base-line spiking oscillations, followed by fast base-line spiking oscillations, sinusoidal Ca^{2+} oscillations and finally non-oscillating signal-plateau Ca^{2+} responses [8]. Of note, Ca^{2+} oscillations occur within a certain range of agonist stimulation. Ryanodine receptors have structural and functional similarity to $InsP_3R$, but show no sensitivity to $InsP_3$ [9]. One of the functions of ryanodine receptors is to amplify the $InsP_3$-mediated release of Ca^{2+} [10]. The unique bell-shaped dependence of $InsP_3R$ and ryanodine receptors on c_{cyt} allow for the repetitive release of Ca^{2+} ions from the endoplasmic reticulum [11]. This is what is observable as Ca^{2+} oscillations.

* Corresponding author at: Anatomy, Department of Medicine, University of Fribourg, Route Albert-Gockel 1, CH-1700 Fribourg, Switzerland.
E-mail address: laszlo.pecze@unifr.ch (L. Pecze).

The transient receptor potential cation channel subfamily V member 1 (TRPV1) triggers intracellular signaling mechanisms by an increase of c_{cyt}, when it is activated by multiple pain-inducing stimuli including heat, acids and pungent compounds [12]. TRPV1 is activated by selective potent natural agonists such as capsaicin (CAPS) and resiniferatoxin (RTX), pungent compounds found in chili pepper and in a tropical plant called *Euphorbia resinifera*, respectively [13]. Upregulation of TRPV1 channels in neoplastic breast and prostate tissue compared to normal tissue has been reported before [14,15], but little is known about the channel's physiological function and the likely pathological consequences in these neoplasms. Virtually all pharmacological and molecular methods used to examine the function of these channels resulted in a decrease of cell viability. These methods included molecular up- or downregulation of the channels and activation or inhibition of channels with natural exogenous agonists or synthetic antagonists [16,17]. The activation of these channels leads to an increase in c_{cyt} in breast and prostate cell lines, but the previously published studies presented only the average of evoked Ca^{2+} cytoplasmic signals within the entire cell populations [17–19]. This method blurs the spatiotemporal character of individual intracellular Ca^{2+} signals, which is essential to understand how TRPV1-mediated stimuli influence the cell behavior at the single cell level.

In this study, spatiotemporal recordings of c_{cyt} and c_{mito} were collected and analyzed; moreover selected mitochondrial functions (membrane potential, ATP production) were analyzed as well. The results revealed the connection between TRPV1 channels and the inositol phospholipid pathway and moreover how TRPV1-mediated Ca^{2+} signals are processed to biologically relevant frequency-modulated Ca^{2+} oscillations. It is known that TRPV1 channels are modulated by phospholipids such as PIP2 [20,21], but our results revealed that the activation of endogenous TRPV1 leads to the production of inositol trisphosphate, thereby reducing the levels of PIP2 in the plasma membrane creating a negative feedback loop.

2. Materials and Methods

2.1. Reagents

Capsaicin (CAPS), a TRPV1 agonist and capsazepine (CapZ), a well-characterized antagonist of TRPV1 were dissolved in DMSO at a concentration of 100 mM (all from Sigma-Aldrich, St. Louis, MO). Resiniferatoxin (RTX) from the LC Laboratories (Woburn, MA) was dissolved in ethanol at a concentration of 2 mM. 13(S)-Hydroxyoctadeca-9Z,11E–dienoic acid (13(S)-HODE), an endogenous agonist of TRPV1 was obtained from Sigma-Aldrich. Suramin from Adipogen (Liestal, Switzerland) was dissolved in double distilled water. Phospholipase C inhibitor U-73122 were from Tocris (Ellisville, MO). The compounds were further diluted with buffer solution used for Ca^{2+}-imaging experiments that contained (in mM): NaCl 138, Na_2PO_4 8, $CaCl_2$ 2, $MgCl_2$ 0.5, KCl 2.7, KH_2PO_4 1.6; pH 7.4. The final concentration of the solvents were <0.1% in all experimental solutions. At these concentrations the solvents did not affect/modify the evoked Ca^{2+} responses in control experiments (data not shown). Ethylene glycol tetra acetic acid (EGTA) was dissolved with NaOH in double distilled water at basic pH (pH > 8.0) and then the pH was adjusted to 7.4 with HCl. The nuclear stain Hoechst 33,342, the mitochondrial marker MitoTracker Red CMXRos and the plasma membrane marker CellMask™-Orange were purchased from Thermo Fisher Scientific Inc. (Waltham, MA).

2.2. Plasmids and cell lines

The cDNA of the human TRPV1 channel (hTRPV1) was amplified from RNA isolated from human trigeminal ganglion tissue as previously described [22]. The pGFP-TRPV1 plasmid resulting in a GFP-TRPV1 fusion protein, as well as the plasmid pTRPV1 encoding full-length TRPV1 were used in this study. The plasmid encoding $InsP_3$ 5-phosphatase (pIRES-InsP3–5P-GFP) was a kind gift from Christophe Erneux, IRIBHM, Bruxelles [23]. The BFP-KDEL plasmid for ER visualization was a gift from Gia Voeltz; Addgene plasmid #49,150. The mCherry-hCdt1 plasmid was a kind gift of Prof. H. Miyoshi (Riken, Japan). This plasmid was used to label nuclei in red color. The control plasmid pEGFP-C1 coding for EGFP was from Clontech (Palo Alto, CA). In order to generate lentivirus encoding the red Ca^{2+} indicator CAR-GECO1 (the CMV-CAR-GECO1 plasmid was a gift from Robert Campbell; Addgene plasmid #45,493), a fragment encoding CAR-GECO1 was cloned into lentiviral expression vector pLVTHM (pLVTHM was a gift from Didier Trono; Addgene plasmid # 12,247)). The GFP cassette in pLVTHM was replaced with cDNAs coding for the respective Ca^{2+} indicator proteins. Briefly, the required cDNA fragment coding for full-length CAR-GECO1 was synthesized by PCR using the primers FW_PmeI_Car-Geco1 (5′- CTT TGT TTA AAC ATG GTC GAC TCA TCA CGT-3′) and RV_*Nde*I_Car-Geco1 (5′-ATT CCA TAT GCT ACT TCG CTG TCA TCA T-3′). The amplicon was digested with *PmeI* and *NdeI* and inserted into the unique sites of the pLVTHM vector to produce the final pLV-CAR-GECO1 plasmid. The lentivirus was produced by the calcium phosphate transfection method using HEK 293 cells and three plasmids: one of the expression plasmids (e.g. pLV-CAR-GECO1 or pLV-mito-CAR-GECO1), the envelope plasmid (pMD2G–VSVG Addgene plasmid #12,259) and the packaging plasmid (psPAX2, Addgene plasmid #12,260). Viral containing supernatants were collected after 48 h and 72 h, filtered, aliquoted and frozen at −80 °C, as described before [24]. Human prostate (PC-3, LNCaP, Du 145) and breast (MCF7, BT-474, MDA-MB-231) cancer cell lines and HEK 293 cells of human embryonic kidney origin were purchased from ATCC (Manassas, VA, USA). Non-transfected NIH-3T3 and rat TRPV1-expressing NIH-3T3 murine fibroblast cells (NIH-3T3^{rTRPV1}) were a kind gift from Dr. Zoltan Olah, University of Miskolc, Hungary. In NIH-3T3^{rTRPV1} cells, the metallothionein promoter is used to drive the expression of full-length rat TRPV1 with a short 12 amino acid ε-tag [25]. Cells were cultivated in DMEM containing 10% fetal calf serum and antibiotics (penicillin and streptomycin) at 37 °C/5% CO_2. DRG primary cultures were prepared from E15 rat embryos as previously described [22]. DRG cell cultures were maintained in DMEM containing 5% horse serum and 100 ng/ml nerve growth factor (Sigma-Aldrich) to promote neuronal survival and differentiation. After 2 days *in vitro* primary DRG cultures were used for the experiments. Du 145 cells stably expressing the Ca^{2+} indicator protein CAR-GECO1 was generated with lentiviral infection. In some experiments, Du 145, MCF7, HEK 293 and NIH-3T3 cells were transiently transfected using the TransIT-2020 transfection reagent according to manufacturer's instructions (Myrus, Madison, WI).

2.3. Immunofluorescence staining

Cells were prepared for immunofluorescence analysis as described previously [26]. As a positive control, MCF7 cells were transiently transfected with plasmids encoding human TRPV1 cDNA. The following antibodies were used for staining: anti-TRPV1 (1:500; rabbit polyclonal, Alomone Labs #ACC-030), Cell nuclei were stained with 5 μg/ml DAPI (Invitrogen) in Tris-buffered saline for 10 min, and mounted with Hydromount solution (National Diagnostics, Atlanta, GA). Images were acquired with a confocal microscope DMI6000 integrated to a Leica TCS-SP5 workstation (Leica, Wetzlar, Germany).

2.4. Ca^{2+} imaging

Cells grown on collagen-coated glass bottom 35 mm dishes (MatTek Corp., Ashland, MA) were loaded with the cell permeable acetoxymethyl (AM)-ester form of the indicator dyes. The following dyes were used: for the cytoplasmic free Ca^{2+} concentration (c_{cyt}): Fluo-4-AM (1 μM; Life Technologies, Grand Island, NY) and for the mitochondrial free Ca^{2+} concentration (c_{mito}): Rhod-2-AM (1 μM; Life Technologies) diluted in cell culture media for 20 min at room temperature. After loading cells

encoded Ca^{2+} indicator CAR-GECO1. At the confocal microscope, fluorescence emission was recorded at 419–474 nm (Hoechst 33342, BFP-KDEL), 510–554 nm (Fluo-4, GFP) and 584 to 683 nm (Rhod-2, CAR-GECO1, MitoTracker Red CMXRos, mCherry-hCdt1) in a sequential mode. Recordings were performed at 37 °C using Tempcontrol 37–*2* digital, and a Heating Stage, all from PeCon GmbH (Erbach, Germany). The drugs were added to the abovementioned solutions by pipette and remained in the solution until the end of the experiments. Fluorescence images for either c_{cyt} or c_{mito} measurements were collected simultaneously. Circular-shaped regions of interest (ROI) were placed inside the cytoplasmic area of cells. The fluorescence values were calculated after background subtraction (fluorescence intensity of regions without cells). Bleaching correction was carried out, when the baseline was not stable. The relative fluorescent unit (F(t)/F(0)) values were calculated for each cell; fluorescence intensities at each time point were divided by the averaged baseline fluorescence value measured during the non-treatment period. In order to gain insight into evoked Ca^{2+} responses of the entire cell population, the traces of >20 randomly selected cells were averaged and standard deviations were calculated (grey traces on figures). Each experimental procedure was repeated at least two times with similar results, but only one series of experiments is reported for each case. The percentage of the responding cells was calculated in each case. The lowest and highest values are presented from the results of three independent experiments. Computerized peak recognition for frequency was realized via the Microsoft Excel 2010 environment as described before [27]; normalized recordings from 20 oscillating cells were evaluated. The oscillation frequency was determined for time window 1–5 min after CAPS administration. The LAS-AF (Leica, Wetzlar, Germany) and Prism3 (GraphPad Software, Inc., San Diego, CA) software were used for data analysis.

2.5. Measurement of mitochondrial function

Mitochondrial membrane potential ($\Delta\Psi$) measurements were performed using the Rhodamine 123 dye. Briefly, cells were seeded on glass-bottom Petri dishes and incubated with 10 μM Rhodamine 123 for 20 min at room temperature. Cells were washed three times with DPBS buffer. During the recording using the confocal microscope, the 488 nm excitation wavelength was used to illuminate Rhodamine 123. The relative mitochondrial membrane potential ($\Delta\Psi$) for a single cell was determined according to the following calculation: the fluorescent intensity of Rhodamine 123 in the cytoplasmic region was divided by that of the nuclear region. Then, the single-cell values were normalized to the average values recorded in the non-treated period (taken as 100% value) and the average values recorded after CCCP treatment (taken as 0% value). The mean and standard deviation were calculated from at least 20 individual cell recordings. Relative ATP levels were determined using the ATP Bioluminescence Assay Kit CLS II (Roche, Basel, Switzerland). Du 145 cells were seeded into a 96-well plate (10,000 cells/well) and grown overnight at 37 °C. The medium was removed and replaced by 100 μl fresh medium containing capsaicin, capsaicin/CCCP or DMSO (equal volume as used for the treatments). After an incubation time of 0, 2 and 5 min, 100 μl 2× passive lysis buffer (Promega, Dübendorf, Switzerland) were added. Samples (50 μl) were pipetted into a black 96-well plate and 50 μl luciferase reagents were added

GFP and $InsP_3$–5 phosphatase or with plasmid encoding only GFP at 50% confluency in 24-well plates. Cells were monitored using the Live Cell Imaging System (Incucyte, EssenBioScience, Michigan, USA) by acquiring images every 1 h. In another experiment, cells were stained with Annexin V-Cy3 (Enzo Life Sciences, Lausen, Switzerland) to identify apoptotic cells following the manufacturer's instruction. Bright field and fluorescent images were collected using an inverted fluorescence microscope DMI6000B (Leica).

3. Results

3.1. Intracellular localization of TRPV1 channels in cancer cell lines

As shown previously [22] all cancer cell lines used in this study express TRPV1 channels evidenced at both, mRNA and protein levels. However, protein expression levels of TRPV1 are much lower in cancer cells than in sensory neurons [22]. Immunofluorescence analysis of TRPV1 expression in prostate and breast cancer cell lines revealed rather homogenous, not mosaic–like expression of TRPV1 in all 6 cell lines. The immunofluorescence signal was mostly localized to intracellular membrane compartments, most prominently in the endoplasmic reticulum (Fig. 1A). Addition of the blocking peptides for the TRPV1 antibodies to the staining solutions resulted in a complete loss of the green immunofluorescence evidenced in MCF7 cells. MCF7 cells overexpressing either human or rat TRPV1 channels served as positive controls; strong green mosaic immunofluorescence was observed in cells overexpressing TRPV1 distinguishing the transfected (strong green fluorescence) from the untransfected ones (Fig. 1A, lower row, right image). The intracellular localization of TRPV1 in living MCF7 cells was visualized by transfection-mediated expression of GFP-labeled TRPV1 receptor. TRPV1 did neither co-localize with mitochondria that were loaded with MitoTracker Red CMXRos nor with cell nuclei labeled with blue Hoechst 33,342 (Fig. 1B, first row). TRPV1 was also clearly expressed on the plasma membrane evidenced by the colocalization of the plasma membrane marker CellMask™-Orange and GFP-TRPV1 (Fig. 1B, second row). Strong colocalization was evident in cells making cell/cell contacts (yellow labeling; arrows). Results from a previous study, i.e. the ability of TRPV1-expressing cells to accumulate $^{45}Ca^{2+}$ ions from the extracellular medium ($^{45}Ca^{2+}$ uptake assay) [22] are in support of the colocalization study that indeed functional TRPV1 channels are present within the plasma membrane. TRPV1 showed co-localization with ER compartments, the latter visualized with blue fluorescent protein having an ER-retention signal, KDEL (Fig. 1B, third row). Nuclei of these cells were visualized with hCdt1-mCherry, a nuclear-localized protein fused to the red fluorescent protein. In some cells (approximately 10% of total cells), possibly representing early apoptotic cells, TRPV1 showed an altered intracellular localization, characterized by a rather homogeneous cytoplasmic, as well as nuclear distribution. These cells had huge vacuolar-like intracellular vesicles and a disorganized ER structure (Fig. 1B, last row).

3.2. Analyses of the CAPS-induced changes in c_{cyt} in carcinoma cell lines

Changes in c_{cyt} were monitored with Fluo-4. Representative c_{cyt} signals for breast cancer cell lines exposed to CAPS (50 μM) are depicted in

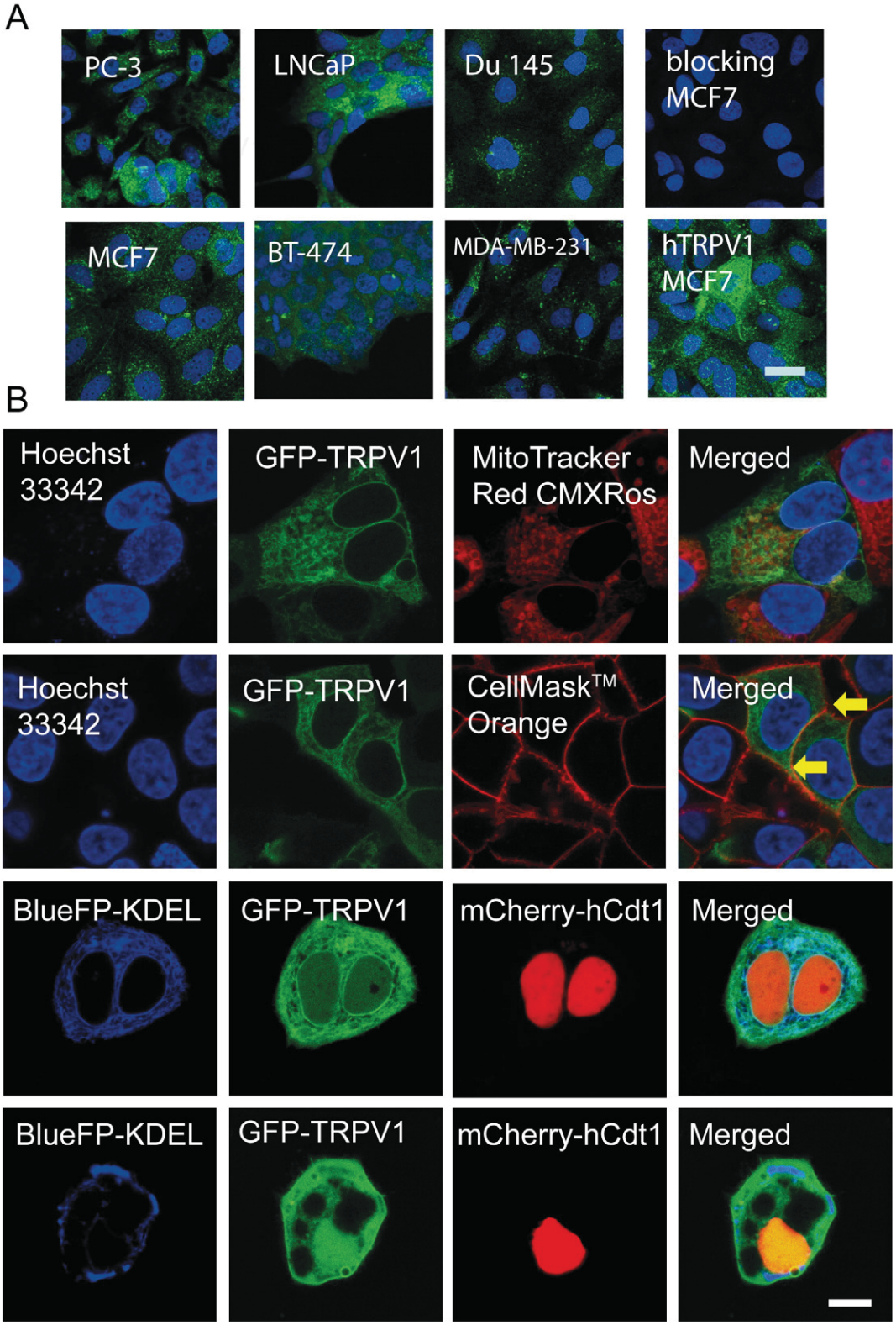

Fig. 1. Expression of TRPV1 channel protein in prostate and breast cancer cell lines. **A**. Immunohistochemical staining for TRPV1 of the 6 cancer cell lines (upper row, prostate cancer cells; lower row, breast cancer cells) showed mostly intracellular localization of TRPV1 channels, likely in ER compartments. Nuclei were counterstained with DAPI. To demonstrate specificity of IHC the TRPV1 antibody was blocked by respective specific peptides in a MCF7 sample (upper row, right). MCF7 cells ectopically expressing human TRPV1 channel were used as positive control (lower row, most right image: bar represents 25 μm). **B.** Fluorescence images show the intracellular localization of GFP-labeled TRPV1 channels in MCF7 cells. TRPV1 doesn't not co-localize with mitochondria: TRPV1 (green), nucleus (blue), mitochondria (red) (first row). TRPV1 present on plasma membranes: TRPV1 (green), nucleus (blue), cell membrane (red) (second row). Strong colocalization at cell/cell contact sites (yellow; arrows). TRPV1 co-localizes with ER compartments in most cells: TRPV1 (green), cell nucleus (red) and ER (blue) (third row). In few cases, TRPV1 shows diffuse cytoplasmic and nuclear staining: TRPV1 (green), cell nucleus (red) and ER (blue) (last row). Bar represent 25 μm.

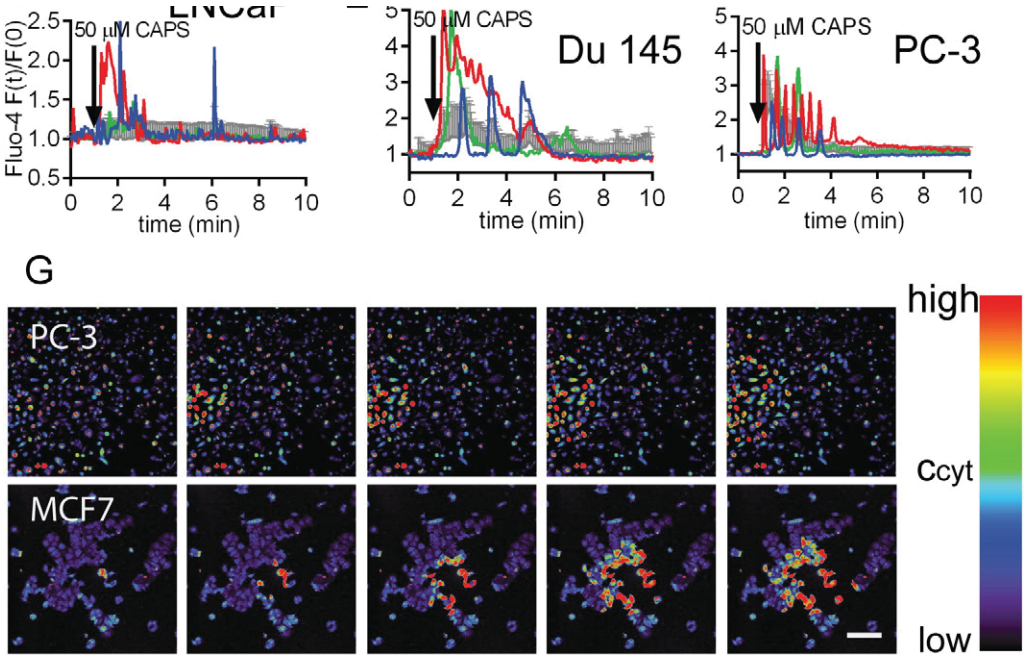

Fig. 2. CAPS-evoked changes in the cytoplasmic free Ca^{2+} concentration (c_{cyt}). A)-F) Single-cell (colored traces) and average fluorescence recordings of the entire cell population (grey traces) from time-lapse videos show changes in c_{cyt} after CAPS administration. Bars represent standard deviations (s.d.). Each figure represents the results of one representative experiment out of three with similar results. Experiments were repeated at least two times with similar results. BT-474 (**A**), MCF7 (**B**) and MDA-MB-231 (**C**) cells treated with CAPS (50 µM) mostly showed immediate onset Ca^{2+} transients; with very brief delays similar increases were observed in neighboring cells often resulting in an intercellular Ca^{2+} wave (**G**). Only very few LNCaP cells (1–3%) responded to CAPS (**D**). CAPS-evoked Ca^{2+} waves and Ca^{2+} oscillations in Du 145 (**E**) and PC-3 (**F**) prostate cancer cells. **G)** Time-lapse image series of intercellular Ca^{2+} waves. The acquisition rate was set to 3 s. Blue and red colors depict lower and higher fluorescence intensities, respectively. A Ca^{2+} wave in PC-3 cells was evoked by administration of 1 µM RTX (upper row). A larger Ca^{2+} wave in MCF7 cells was evoked by 50 µM CAPS (lower row). Bar represents 150 µm.

derived cell lines responded to CAPS administration with rapid increases in c_{cyt} often followed by intracellular Ca^{2+} oscillations (Fig. 2D-F). In PC-3 (prostate) and MCF7 (breast) cancer cells, the stimulation with 1 µM RTX or 50 µM CAPS, respectively, additionally resulted in intercellular Ca^{2+} waves (Fig. 2G). Ca^{2+} waves spreading through cultured cells were either seen immediately after CAPS administration or occasionally few minutes later. In the case of MCF7 cells, the area covered by the waves was sometimes restricted to only few adjacent cells, but in sporadic occasions waves spread almost over the entire cell population in the observed area (772 × 772 µm). The Ca^{2+} wave velocity was rather similar in both cell lines, 13.4 ± 3.2 µm/s in PC-3 cells and 11.0 ± 3.3 µm/s in MCF7 cells (Fig. 2G). Since LNCaP and BT-474 cells grew in aggregates (i.e. on top of each other), Ca^{2+} waves could not be examined in our experimental setting. The percentage of the responding cells varied quite strongly between cell lines and also between experiments using the same cell lines: PC-3 (56–75%), LNCaP (1–3%), Du 145 (65–72%) and breast MCF7 (5–71%), BT-474 (11–23%) and MDA-MB-231 (21–49%). A more detailed statistical analysis is presented in the Supplementary Materials.

3.3. Mechanistic characterization of CAPS-evoked Ca^{2+} oscillations in Du 145 cells

in the generation of these oscillations were investigated in more detail. Ca^{2+} transients in Du 145 were also elicited by 5 µM 13-S-hydroxyoctadecadienoic acid (13-HODE; Supplementary Fig. S1), an endogenous but weak agonist of TRPV1 resulting in 25–34% responding cells (Fig. 3A). Moreover the ultrapotent and specific TRPV1 agonist RTX (1 µM) also evoked Ca^{2+} signals in Du 145 cells (31–44% responding cells; Fig. 3B). The selective and full antagonist of TRPV1 channels, CapZ (100 µM), nearly completely inhibits TRPV1-mediated Ca^{2+} signals evoked by 5 µM CAPS in a heterologous expression system [29]. Similarly, CAPS (5 µM) evoked Ca^{2+} signals in Du 145 cells; however the average signal was smaller than that evoked by 50 µM CAPS (27–33% responding cells) and the oscillations immediately halted or the frequency was highly reduced after CapZ (10 µM) administration (Fig. 3C). When CapZ (100 µM) was administered before agonist stimulation, CAPS-evoked responses were strongly reduced (Fig. 3D; only approximately 2–5% responding cells). CapZ also blocked around 45–60% of spontaneous Ca^{2+} oscillations observable in 3–5% of Du 145 cells (Supplementary Fig. S2). Ca^{2+} oscillations were dependent on phospholipase C activation, since the addition the phospholipase C inhibitor U-73122 blocked the CAPS-evoked oscillations in Du 145 cells (Fig. 3E). When cells were pre-treated with 50 µM U-73122, CAPS treatment didn't induce oscillations, only single Ca^{2+} transients were observed in 14–22% of cells (Fig. 3F). Activation of phospholipase C results in

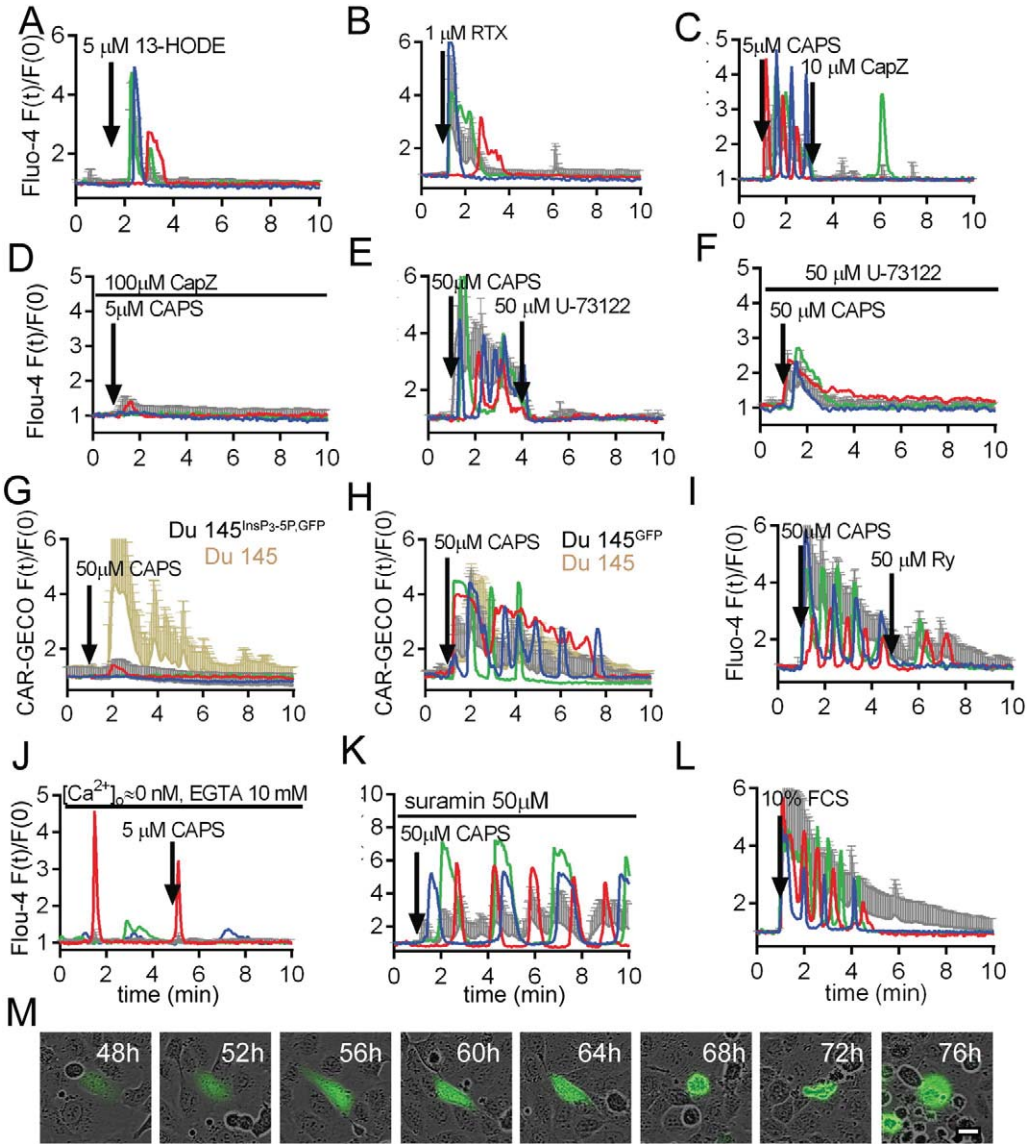

Fig. 3. The effect of simultaneous administration of TRP agonists. A)-L) Single-cell (colored traces) and average fluorescence (grey traces) recordings from time-lapse videos show changes in c_{cyt}. Bars represent standard deviations (s.d.). Each figure represents the results of one representative experiment out of three with similar results. **A)** 13-HODE (5 μM), an endogenous TRPV1 agonist, evoked weak Ca^{2+} responses. **B)** Ca^{2+} responses were evoked by administration of 1 μM RTX, a specific potent TRPV1 agonist. **C)** CapZ, a TRPV1 blocker, administered after CAPS stopped or strongly decreased the frequency of CAPS-evoked Ca^{2+} oscillations in Du 145 cells. **D**) CapZ administered before CAPS strongly reduced the CAPS-evoked response **E)** U-73,122, a phospholipase C inhibitor, blocked the CAPS-evoked Ca^{2+} oscillations. **F)** Cells pre-treated with 50 μM U-73122f didn't showed oscillations. **G)** Overexpression of $InsP_3$–5-phosphatase hydrolyzing $InsP_3$ concomitant with GFP protein expression inhibited CAPS-induced oscillations (single cell recordings in red, blue and green color). Grey and yellow traces represents average fluorescence recordings from cells with or without $InsP_3$-hydrolysing enzyme from the same culture dish, respectively **H)** GFP expression alone had no effect on oscillations (single cell recordings in red, blue and green color). Grey and yellow traces represents average fluorescence recordings from cells with or without GFP from the same culture dish, respectively **I**) Ryanodine (50 μM) transiently inhibited the Ca^{2+} oscillations. **J)** In the absence of external Ca^{2+} ions CAPS did not induce Ca^{2+} responses, but some spontaneous Ca^{2+} oscillations were still observable **K)** Suramin, a blocker of purinergic receptors, decreased the frequency of Ca^{2+} oscillations. **L)** Serum re-administration to Du 145 cells evoked Ca^{2+} oscillations similar to responses to CAPS administration. **M**) Time-lapse recording of Du 145 cells transfected with GFP-labeled $InsP_3$–5-phosphatase. Most of transfected cells show the morphological appearance of apoptosis: cell shrinkage, nuclear condensation, blebs and detachment from surface. Bar represents 20 μm.

consider that both activation and inhibition of phospholipase C has an effect on the phospholipid composition of the plasma membrane that subsequently influences the sensitivity of TRPV1 channels [20,21]. The importance of $InsP_3$ in the generation of Ca^{2+} oscillations was further verified by overexpression of the $InsP_3$-metabolizing enzyme $InsP_3$–5 phosphatase. When the enzyme was expressed from a GFP polycistronic construct, the GFP expression enabling the identification of transfected $InsP_3$–5 phosphatase-producing cells, CAPS was still able to generate small Ca^{2+} signals in 12–14% of GFP-positive cells (Fig. 3G). However, Ca^{2+} oscillations completely disappeared. The non-transfected GFP-negative neighbors showed regular oscillations (62–75% responding cells) (Fig. 3G, yellow trace). In a control experiment, cells only expressing GFP showed oscillations indicating the GFP by itself had no effect on the appearance of Ca^{2+} oscillations (Fig. 3H). Ryanodine (50 μM) caused a brief block of the CAPS-evoked Ca^{2+} oscillations indicative of the importance of ryanodine-sensitive stores for the maintenance of oscillations in these cells (Fig. 3I). Importantly, the removal of extracellular Ca^{2+} strongly diminished and in most cases abolished the CAPS-evoked TRPV1-mediated effects; while the CAPS-induced immediate increase in c_{cyt} was essentially absent, spontaneous oscillations in few cells (1–2%) were insensitive to extracellular Ca^{2+} elimination by high external EGTA (10 mM) (Fig. 3J). Extracellular ATP (5 μM) also evoked Ca^{2+} oscillations in 83–91% of Du 145 cells (Supplementary Fig. S3), which were partially inhibited by 50 μM suramin, a blocker of ATP-sensing purinergic receptors (Supplementary Fig. S4). Extracellular release of ATP had been found to play an important role in generation of

inositol phospholipid pathway [27,32]. This procedure applied to Du 145 cells resulted in the generation of similar oscillations in c_{cyt} (80–95% responding cells), as was observed after CAPS treatment (Fig. 3L). Cells transfected with a plasmid encoding both GFP and $InsP_3$–5 phosphatase were monitored. After 72 h, approximately 30–40% of transfected cells showed the morphological signs of apoptosis: cell shrinkage, nuclear condensation, membrane blebs, cell detachment from the culture plate and appearance of apoptotic bodies (Fig. 3M). These cells were also positive to Annexin V-Cy3 red staining (apoptosis indicator) (Supplementary Fig. S5, upper row). In a control experiment cells were transfected with the plasmid pEGFP-C1 encoding only GFP protein. Clearly less cells, approximately 5% of transfected cells were positive for Annexin V-Cy3 staining (Supplementary Fig. S5, lower row). Our finding that blocking of the Ca^{2+} oscillations by $InsP_3$–5 phosphatase overexpression reduced cell viability indicates that the inositol phospholipid pathway plays an important role in the physiology of Du 145 cells.

3.4. Increase in c_{mito} leads to ATP production in CAPS-treated Du 145 cells

In hepatocytes and primary mesothelial cells oscillations in c_{cyt} activate mitochondrial enzymes and also augment mitochondrial function [32,33]. Although ATP production in cancer cells is mainly based on aerobic glycolysis, mitochondria are implicated in ATP production also in tumor cells [34]. The oscillations in c_{cyt} evoked by CAPS resulted in concomitant changes in the free mitochondrial matrix Ca^{2+} concentration (c_{mito}) (Fig. 4A). As observed before in mesothelial cells [32], the changes in c_{mito} occurred with a small time delay compared to the c_{cyt} signals (Fig. 4A). The addition of CAPS also slightly increased the mitochondrial membrane potential ($\Delta\Psi$), however the increase was not significant (Fig. 4B). In comparison to untreated cells, CAPS treatment resulted in a small, yet significant increase in ATP production in Du 145 cells, evidenced by a side-by-side comparison of untreated vs. CAPS-treated Du 145 cells measured 2 and 5 min after CAPS addition (Fig. 4C). Collapsing of the mitochondrial membrane potential by the uncoupler carbonyl cyanide m-chlorophenyl hydrazone (CCCP; Fig. 4B)) diminished ATP production despite the concomitant presence of the TRPV1 agonist CAPS (Fig. 4C).

3.5. CAPS treatment of DRG neurons but not of NIH-3 T3 cells ectopically expressing TRPV1 results in Ca^{2+} oscillations

Recently, we have demonstrated that DRG neurons express higher levels of TRPV1 channels than cancer cells. Moreover, activation of sensory neurons with 20 μM CAPS leads to overstimulation-based cytotoxicity in sensory neurons with signal plateau-type responses in c_{cyt} [22,35]. Yet at lower CAPS concentrations in the range of 1 μM approximately 30–40% of DRG neurons showed Ca^{2+} oscillations (Fig. 5A). Similar experiments were carried out in NIH-3T3 cells characterized by very low to none endogenous TRPV1 expression [25] and treatment with 50 μM CAPS had no effect on c_{cyt} (0% of responding cells) (Fig. 5B). When these cells were transfected with plasmids coding for either human or rat TRPV1 channels, addition of CAPS (50 μM) resulted in rapid signal-plateau Ca^{2+} responses in 15–28% of cells, thus allowing to quickly identifying the transfected (TRPV1+) subpopulation of

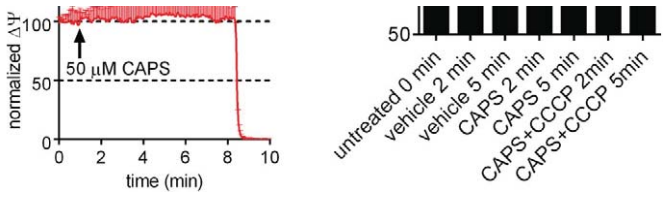

Fig. 4. CAPS-mediated cytoplasmic Ca^{2+} oscillations in Du 145 cells lead to increases in c_{mito} and ATP synthesis A) Simultaneous measurement of c_{cyt} and c_{mito} revealed that oscillations in c_{cyt} led to oscillations in c_{mito} with a slight time delay. A representative recording of c_{cyt} (green) and c_{mito} (red) in a Du 145 cell is shown. **B)** Oscillations in c_{mito} slightly increased the mitochondrial potential ($\Delta\Psi$), which collapsed after administration of 100 μM CCCP. Figure represents the results of one representative experiment out of three with similar results. **C)** Upon CAPS stimulation ATP production was significantly increased 2 and 5 min after stimulation compared to vehicle-treated cells. CAPS (50 μM) administration in the presence of the uncoupler CCCP (500 μM) resulted in decreased ATP production compared to the vehicle-treated cells. Each column represents the result of >10 independent samples (mean ± s.d.). Significant differences between samples are marked with * ($p < 0.05$).

end of the experiment. Cells were first treated with a low CAPS concentration (50 nM), followed by 50 μM CAPS several minutes later. In all responding cells one of the four following patterns were observed: Type I) In 2–3% of cells, strong signal-plateau Ca^{2+} responses were observed already after administration of 50 nM CAPS (e.g. green trace in Fig. 5C), most probably indicative of high levels of ectopic TRPV1 expression. Type II) In 9–15% of cells, after a weak and prolonged Ca^{2+} increase evoked by 50 nM CAPS, c_{cyt} slowly recovered to baseline levels, usually within 5–7 min after treatment. This was followed by strong signal-plateau responses evoked by 50 μM CAPS (e.g. red trace in Fig. 5C). Type III) Cells (6–11%) didn't respond to low CAPS exposure, but displayed strong responses to high CAPS concentration (e.g. blue trace in Fig. 5C). Type IV) Cells (72–85%) that didn't respond to 50 μM CAPS were assumed to comprise the TRPV1- subpopulation (e.g. orange trace in Fig. 5C). Of note in all conditions, no Ca^{2+} oscillations were observable. Essentially identical results were obtained, when cells stably overexpressed rat TRPV1. The same four behaviors towards low and high CAPS exposure were observed (Type I, Type II, Type III and Type IV responses in 24–30%, 43–52%, 17–26% and 1–5% of cells, respectively) and these cells showed neither spontaneous nor CAPS-evoked Ca^{2+} oscillations. (Fig. 5D). Thus, these results indicated that overexpression of TRPV1 alone is not sufficient to produce Ca^{2+} oscillations. Circumventing the need for TRPV1 signaling by transient serum withdrawal followed by serum re-administration resulted in clear Ca^{2+} oscillations in NIH-3T3 cells (80–90% of responding cells; Fig. 5E), which was strongly blocked by U-73122 pre-treatment (Fig. 5F). This indicated that the inositol phospholipid pathway is indeed intact in NIH-3T3 cells, but that stimulation of ectopic TRPV1 was unable to induce this activation. The reason for this may be manifold; one possibility is that TRPV1 is associated with a linker protein required to indirectly activate the inositol phospholipid pathway. Of note, ectopic human TRPV1-expressing NIH-3 T3 cells stimulated with 50 μM CAPS showed a long-lasting Ca^{2+} signal resembling the one evoked by the Ca^{2+} ionophore ionomycin (Fig. 5G). The ionomycin treatment (100% responding cells) rendered both plasma and ER membranes permeable for Ca^{2+} ions, but also did not link the c_{cyt} increase to the activa-

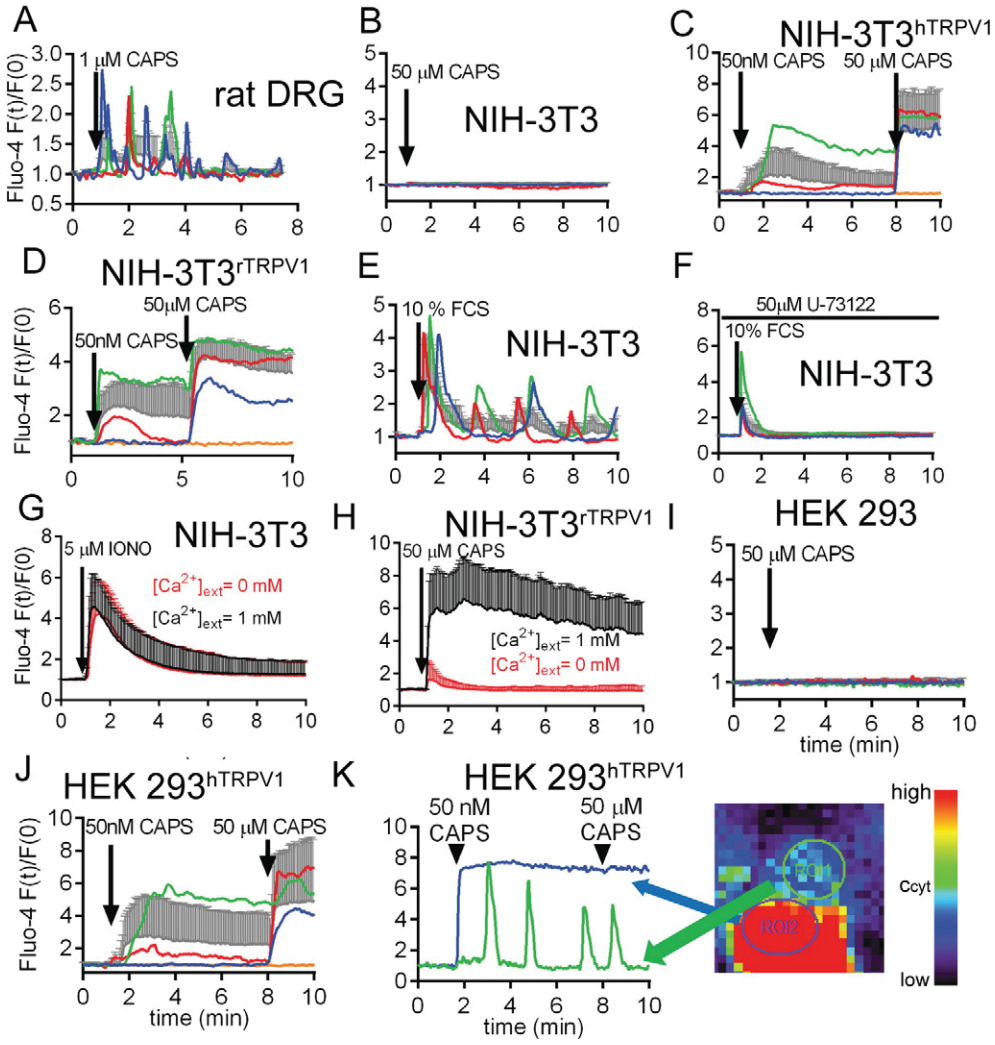

Fig. 5. CAPS-mediated Ca^{2+} signals in DRG sensory neurons and in NIH-3 T3 cells ectopically expressing TRPV1 A)-E) Single-cell (colored traces) and average fluorescence (grey traces) recordings from time-lapse videos show changes in c_{cyt}. Bars represent standard deviations (s.d.). Each figure represents the results of one representative experiment out of three with similar results. **A)** A subset of cultured rat DRG neurons showed Ca^{2+} oscillations after CAPS (1 μM) treatment. **B)** Non-transfected NIH-3T3 cells do not respond to 50 μM CAPS. **C**) Ectopic expression of human TRPV1 rendered NIH-3T3 cells extremely sensitive to CAPS resulting in signals already at 50 nM CAPS and even higher ones with 50 μM CAPS. No oscillations were observed. **D)** Similar low magnitude, long-lasting elevations of c_{cyt}, instead of Ca^{2+} oscillations, were observed when rat TRPV1 was ectopically overexpressed. **E)** Ca^{2+} oscillations appeared when serum was re-administered to NIH-3 T3 cells. **F)** U-73,122 pre-treatment significantly reduced the serum evoked response **G**) Ionomycin treatment didn't result in Ca^{2+} oscillations and showed similar Ca^{2+} signals in the presence (black) or absence (red) of extracellular Ca^{2+}. **H)** In the presence of extracellular Ca^{2+} ions (black trace) the Ca^{2+} response after CAPS treatment was more pronounced in TRPV1-expressing NIH-3T3 cells in comparison to control cells maintained in the absence of extracellular Ca^{2+} (red trace). **I**) Non-transfected HEK 293 cells didn't respond to 50 μM CAPS. **J**) Low or high magnitude, long-lasting elevations of c_{cyt}, but not Ca^{2+} oscillations were usually observed when human TRPV1 was ectopically overexpressed in HEK 293 cells. **K)** Few likely non-transfected HEK 293 cells (green traces), mainly in the neighborhood of a highly sensitive transfected HEK 293 cell (blue curve) showed Ca^{2+} oscillations.

TRPV1-mediated and ionomycin-induced elevations in c_{cyt} was their dependence on extracellular Ca^{2+}. The ionomycin-evoked increase in c_{cyt} didn't differ much, whether extracellular Ca^{2+} was high or low (Fig. 5G) indicating that the majority of Ca^{2+} ions leading to the transient increase in c_{cyt} was derived from internal stores. The TRPV1-mediated CAPS-induced Ca^{2+} signal was significantly smaller in low extracellular Ca^{2+} conditions indicative of an essential contribution of plasma membrane-located TRPV1 in the increase of c_{cyt} (Fig. 5H). However, irrespective of the Ca^{2+} source (internal store, extracellular) the robust increase in c_{cyt} was not leading to oscillations. HEK 293 cells, similarly to NIH-3T3 cells, are characterized by very low to none endogenous TRPV1 expression [36]. These cells didn't respond to CAPS treatment (Fig. 5I). Overexpression of TRPV1 channels resulted in the same four behaviors towards low and high CAPS exposure observed before in NIH-3T3 (Type I, Type II, Type III and Type IV responses in 15–38%, 15–27%, 13–21% and 18–32% of cells, respectively (Fig. 5J). However approximately 5–13% of cells showed Ca^{2+} oscillations or single Ca^{2+} spikes after 50 nM CAPS stimulation. Since these oscillating cells didn't respond to high CAPS (50 μM) with constant elevated c_{cyt}, we presume that these cells consisted of non-transfected cells. Of note, those cells were always next neighbors of a highly sensitive TRPV1-expressing cells (Fig. 5K). Currently we can't provide a clear explanation for this finding. We hypothesize that TRPV1-expressing highly-sensitive cells might release some agonist molecule(s) that affect the oscillatory behavior of a neighboring TRPV1-negative cell.

4. Discussion

Activation of TRPV1 channels by endogenous compounds or pharmacological substances such as CAPS may lead to various biological responses in different cell types. Mild TRPV1 activation leads to proliferation of airway smooth muscle cells [37] and is involved in the induction of skeletal muscle hypertrophy [38]. TRPV1 expression in sensory neurons is associated with pain and heat sensation [39]. Strong and persistent activation of TRPV1 on sensory neurons leads to the elimination of TRPV1-expressing neurons due to overstimulation-based cytotoxicity

found that production of $InsP_3$ and continuous Ca^{2+} influx across the plasma membrane are two essential and frequency-determining factors for Ca^{2+} oscillations.

Prostate and breast cancer cells, previously shown to express *TRPV1* transcripts and TRPV1 protein [22], produced CAPS-induced Ca^{2+} waves and Ca^{2+} oscillations. CAPS is a selective TRPV1 receptor agonist with a half-maximal effective concentration for CAPS in sensory neurons in the range of 200–700 nM [42,43]; CAPS evokes Ca^{2+} signals at low nanomolar concentrations in heterologous expression systems. In line, NIH-3 T3 cells overexpressing TRPV1 responded to 50 nM CAPS with increases in c_{cyt} (Figs. 5C, D). However, a concentration of at least 5–50 μM CAPS was required to elicit Ca^{2+} responses in the untransfected prostate and breast cancer cells. The lower CAPS sensitivity of cancer cells is likely linked to the lower TRPV1 expression levels in these cells in comparison to TRPV1-expressing sensory neurons, estimated to be at least 20-fold lower in the investigated cancer cell lines [22]. Of relevance, the concentrations (5 μM and 50 μM) used in this study were still below the concentration, where an unspecific effect of CAPS was reported before. CAPS (250 μM and higher) blocks the respiratory chain acting as a quinone analog [44]. CAPS-evoked responses were inhibited by administration of CapZ, a genuine and competitive TRPV1 agonist. Moreover, the ultrapotent and highly specific TRPV1 agonist RTX and one of the endogenous TRPV1 agonists, 13-HODE, also generated Ca^{2+} signals indicating the involvement of TRPV1 channels in the process. In sensory neurons, exposure to 1 μM CAPS was sufficient

nel activation leads to $InsP_3$ production is currently unknown; however some hypotheses can be put forward. I) Activation of phospholipase C by TRP channels is induced by Ca^{2+} ions transported by the TRP channels, as the activity of phospholipase C depends on increases in c_{cyt} as reported before [45]. Since merely an increase in c_{cyt} did not lead to Ca^{2+} oscillations (Fig. 5B, C, E and F), we can conclude that this process does not play a critical role in phospholipase C activation. However, the transport of Ca^{2+} ions across the plasma membrane is important for the maintenance of Ca^{2+} oscillations and also affecting the oscillation frequency [27,32]. Thus, the amount of Ca^{2+} ions passing through TRPV1 channels sustains Ca^{2+} oscillations and influences the oscillation frequency (Fig. 3C, D). II) TRPV1 channels are associated with G proteins and upon stimulation, G proteins activate phospholipase C; an association between TRPM8, another TRP family member, and $G_{\alpha q}$ proteins has been described before [46]. The direct connection between TRPV1 and G proteins has to be elucidated in a future study. III) Previous experiments in astrocytes and hepatocytes [30,31] indicate that ATP is the molecule released by the wave-initiator cells. ATP binding to purinergic receptors on neighboring cells then results in $InsP_3$ production required for the generation of Ca^{2+} oscillations and intercellular Ca^{2+} waves. In analogy, we hypothesize that TRP channel stimulation might induce extracellular ATP release, followed by $InsP_3$ production in neighboring cells resulting in Ca^{2+} signals in those cells. In support, the purinergic receptor blocker suramin, effective in blocking of ATP-evoked Ca^{2+} oscillations, was not effective in blocking of the CAPS-induced oscillations,

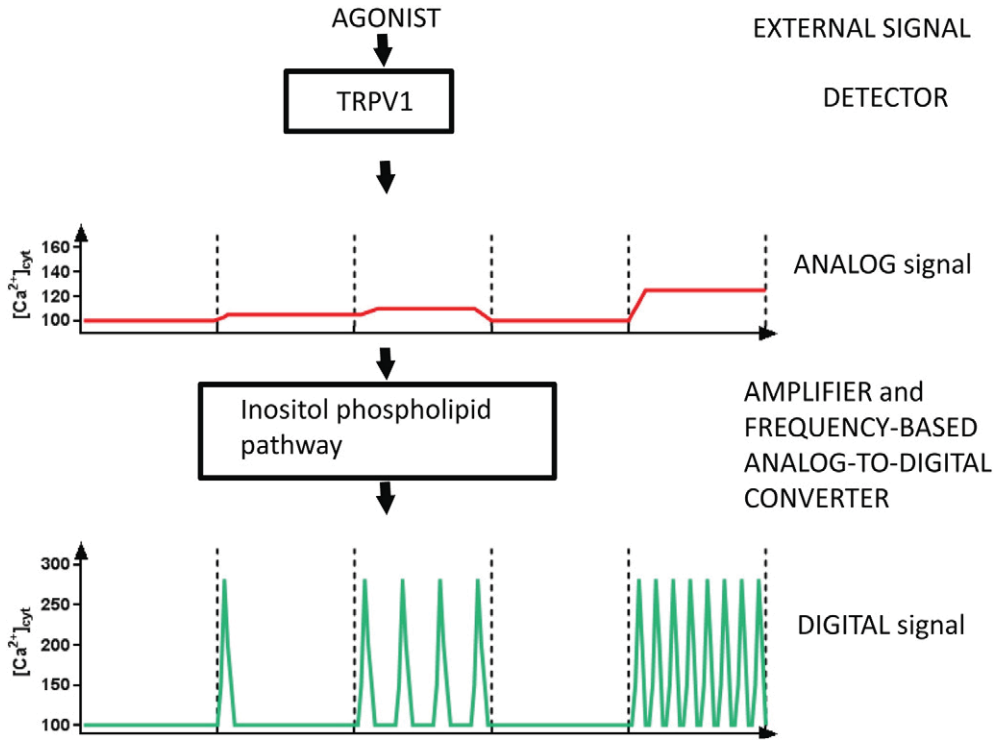

Fig. 6. Proposed model for the role of TRPV1 channels in signal transmission. The observed CAPS-evoked Ca^{2+} signal is mainly the result of the activated phospholipid pathway

but reduced the Ca^{2+} oscillation frequency and more importantly, Ca^{2+} wave formation.

Although in this study we focused on the effect of TRPV1 activation on the phospholipid pathway, it is known that phospholipids themselves also modify the sensitivity and function of TRPV1 channels. Phosphatidylinositol 4,5-bisphosphate (PIP2), a precursor molecule for the $InsP_3$ production was found to sensitize TRPV1 channels to CAPS. Besides of that, also phosphatidylinositol 4-phosphate PI(4)P was found to sensitize the receptor [47]. Moreover, the depletion of PIP2 from the plasma membrane, either alone or together with PI(4)P inhibits TRPV1 channel function [47,48]. This process was shown to be involved in the mechanism of TRPV1 desensitization [47]. Thus, we propose the following negative feedback loop for TRPV1 regulation: TRPV1 channel activity leads to phospholipase C activation, which, in turn, slowly depletes PIP2 and PI(4)P from the membrane. This depletion then leads to the inhibition of TRPV1 receptor resulting in a halt of the Ca^{2+} oscillations.

To get more mechanistic insight in TRPV1-mediated Ca^{2+} responses, we chose Du 145 prostate cancer cells. TRPV1 was involved both in the induction and the maintenance of Ca^{2+} oscillations, i.e. by generating $InsP_3$ and mediating Ca^{2+} influx via the plasma membrane. The frequency of Ca^{2+} oscillations is implicated in regulating genes driven by pro-inflammatory transcription factors such as NF-κB, NF-AT and Oct./OAP [49]. Ca^{2+} oscillations were shown to activate Ras and ERK/MAPK cascades controlling cell growth and differentiation [50]. Moreover, Ca^{2+} oscillations induce ATP production energizing many cellular processes [51]. In this study we also found that Ca^{2+} oscillations energized the mitochondria in Du 145 cells. Although the abovementioned physiological processes are associated with increased cell viability and mitogenic processes, there are only few studies reporting that CAPS increase cell proliferation of cancer cells. While CAPS (50 μM) increases the proportion of cells present in the G_2 phase, the proportion of G_0/G_1 cells is decreased compared to control (untreated) LNCaP cells [52]. Similarly Malagarie-Cazenave et al. found that CAPS induced cell proliferation in LNCaP prostate cancer cells in the same concentration range [53]. We also reported that 5–50 μM CAPS treatment slightly, but in many cases significantly increases the cell proliferation of breast and prostate cancer cells *in vitro* [22]. Besides of that, we also reported CAPS-induced invadopodium formation in MCF7 breast cancer cells [22]. Invadopodium is an amoeboid-like structure involved in tumor cell motility [54].

Endogenous agonists of TRPV1 channels such as arachidonyl acid derivatives and oxidized linoleic acid metabolites are present in the tumor milieu [55]. It has been known for a long time - even before TRP channels were discovered - that endogenous agonists of TRP channels (lipoxygenase products) promote tumor growth [56]. However, the experimental evidence that the mitogenic, growth-promoting effects of lipoxygenase products are mediated by TRPV1 has never been described before. The oxidized linoleic acid metabolite 13-S-hydroxyoctadecadienoic acid (13-HODE) was observed in human prostate adenocarcinoma specimens, whereas adjacent normal tissue showed no immunoreactivity for 13-HODE [57]. Similarly, a low pH in the extracellular milieu, another activator of TRPV1 [58], is also associated with inflammation and the cancer microenvironment [59,60]. LNCaP cells produce high amounts of 20-hydroxyeicosatetraeonic acid (20-HETE) [61], another endogenous activator of TRPV1 channels [62]. Expression of 12-lipoxygenase, the enzyme involved in generation of 12(*S*)-hydroxyeicosatetraeonic acid (12-HETE), was found to correlate with more malignant stages of prostate cancer [63,64]. 12-HETE is an endogenous TRPV1 ligand known to increase the firing rate of sensory neurons via TRPV1 activation [65]. Most probably, the TRPV1 channel is the "putative G protein linked receptor [55]" involved in the proliferative effect of the lipoxygenase pathway product.

In summary, endogenous TRPV1 channels are connected with the inositol phospholipid pathway. The observed CAPS-evoked Ca^{2+} signals are the result of the activated phospholipid pathways and not only the Ca^{2+} ions passing through the TRPV1 channels. Since TRPV1 channels alone cannot produce Ca^{2+} oscillations, the analog amplitude-modulated (AM) increase in c_{cyt} is processed by inositol phospholipid pathway. The inositol phospholipid pathway acts as an amplifier and "analog to digital converter" to generate the frequency-modulated (FM) output (Ca^{2+} oscillations) for a given Ca^{2+} signal produced by TRPV1 activation (for details, see model in Fig. 6). In cancer cells, one might envisage the following pathophysiological processes: increased levels of endogenous agonists present in the cancer microenvironment activate TRPV1 channels; the resulting Ca^{2+} influx via TRP channels together with increased $InsP_3$ production induces Ca^{2+} oscillations and these Ca^{2+} oscillations (FM mode) activate Ca^{2+} signaling-dependent transcription factors involved in cell proliferation. I.e. auto- or paracrine TRPV1 channel activation in cancer cells might promote their survival and possibly increase their proliferation rate *in vivo*.

Authors contributions

LP designed the study, performed Ca^{2+} measurements, data analysis and wrote the manuscript HT performed ATP measurements WB performed cloning and plasmid production and apoptosis assay BS performed data analyses and wrote the manuscript and secured funding.

Conflict of interest statement

The authors declare that they have no conflicts of interest with the contents of this article.

Transparency document

The Transparency document associated with this article can be found, in online version.

Acknowledgements

The authors wish to thank Valérie Salicio and Martine Steinauer for excellent technical assistance as well bachelor students Alessio Balmelli and Chantal Bachmann for their assistance. This work has been supported by Swiss National Science Foundation SNSF grant # 130680 to B.S.

Appendix A. Supplementary data

Supplementary data to this article can be found online at http://dx.doi.org/10.1016/j.bbamcr.2016.09.013.

References

[1] A.M. Dolmetsch, Nonlaser endoscopic endonasal dacryocystorhinostomy with adjunctive mitomycin C in nasolacrimal duct obstruction in adults, Ophthalmology 117 (2010) 1037–1040.
[2] T. Ishiguro, K. Ishikawa, M. Takahashi, M. Obayashi, T. Amino, N. Sato, M. Sakamoto, H. Fujigasaki, F. Tsuruta, R. Dolmetsch, T. Arai, H. Sasaki, K. Nagashima, T. Kato, M. Yamada, H. Takahashi, Y. Hashizume, H. Mizusawa, The carboxy-terminal fragment of alpha(1A) calcium channel preferentially aggregates in the cytoplasm of human spinocerebellar ataxia type 6 Purkinje cells, Acta Neuropathol. 119 (2010) 447–464.
[3] L. Munaron, Calcium signalling and control of cell proliferation by tyrosine kinase receptors (review), Int. J. Mol. Med. 10 (2002) 671–676.
[4] R.E. Dolmetsch, R.S. Lewis, C.C. Goodnow, J.I. Healy, Differential activation of transcription factors induced by Ca2 + response amplitude and duration, Nature 386 (1997) 855–858.
[5] M.J. Berridge, Neuronal calcium signaling, Neuron 21 (1998) 13–26.
[6] K. Mikoshiba, Role of IP3 receptor signaling in cell functions and diseases, Adv. Biol. Regul. 57 (2015) 217–227.
[7] M. Yamashita, 'Quantal' Ca(2 +) release reassessed–a clue to oscillation and synchronization, FEBS Lett. 580 (2006) 4979–4983.
[8] G. Bidaux, M. Flourakis, S. Thebault, A. Zholos, B. Beck, D. Gkika, M. Roudbaraki, J.L. Bonnal, B. Mauroy, Y. Shuba, R. Skryma, N. Prevarskaya, Prostate cell differentiation status determines transient receptor potential melastatin member 8 channel subcellular localization and function, J. Clin. Invest. 117 (2007) 1647–1657.

163–173.
[14] I. Azimi, S.J. Roberts-Thomson, G.R. Monteith, Calcium influx pathways in breast cancer: opportunities for pharmacological intervention, Br. J. Pharmacol. 171 (2014) 945–960.
[15] G. Czifra, A. Varga, K. Nyeste, R. Marincsak, B.I. Toth, I. Kovacs, L. Kovacs, T. Biro, Increased expressions of cannabinoid receptor-1 and transient receptor potential vanilloid-1 in human prostate carcinoma, J. Cancer Res. Clin. Oncol. 135 (2009) 507–514.
[16] T.T. Wu, A.A. Peters, P.T. Tan, S.J. Roberts-Thomson, G.R. Monteith, Consequences of activating the calcium-permeable ion channel TRPV1 in breast cancer cells with regulated TRPV1 expression, Cell Calcium 56 (2014) 59–67.
[17] C. Vercelli, R. Barbero, B. Cuniberti, S. Racca, G. Abbadessa, F. Piccione, G. Re, Transient receptor potential vanilloid 1 expression and functionality in mcf-7 cells: a preliminary investigation, J. Breast Cancer 17 (2014) 332–338.
[18] E. Sakalli Cetin, M. Naziroglu, B. Cig, I.S. Ovey, P. Aslan Kosar, Selenium potentiates the anticancer effect of cisplatin against oxidative stress and calcium ion signaling-induced intracellular toxicity in MCF-7 breast cancer cells: involvement of the TRPV1 channel, J. Recept. Signal Transduct. Res. (2016) 1–10.
[19] B. Cig, M. Naziroglu, Investigation of the effects of distance from sources on apoptosis, oxidative stress and cytosolic calcium accumulation via TRPV1 channels induced by mobile phones and Wi-Fi in breast cancer cells, Biochim. Biophys. Acta 1848 (2015) 2756–2765.
[20] E. Hernandez-Garcia, T. Rosenbaum, Lipid modulation of thermal transient receptor potential channels, Curr. Top. Membr. 74 (2014) 135–180.
[21] T. Rohacs, Phosphoinositide regulation of TRPV1 revisited, Pflugers Arch. 467 (2015) 1851–1869.
[22] L. Pecze, K. Josvay, W. Blum, G. Petrovics, C. Vizler, Z. Olah, B. Schwaller, Activation of endogenous TRPV1 fails to induce overstimulation-based cytotoxicity in breast and prostate cancer cells but not in pain-sensing neurons, Biochim. Biophys. Acta 1863 (2016) 2054–2064.
[23] G. Tran Van Nhieu, B. Kai Liu, J. Zhang, F. Pierre, S. Prigent, P. Sansonetti, C. Erneux, J. Kuk Kim, P.G. Suh, G. Dupont, L. Combettes, Actin-based confinement of calcium responses during Shigella invasion, Nat. Commun. 4 (2013) 1567.
[24] W. Blum, B. Schwaller, Calretinin is essential for mesothelioma cell growth/survival in vitro: a potential new target for malignant mesothelioma therapy? Int. J. Cancer 133 (2013) 2077–2088.
[25] Z. Olah, T. Szabo, L. Karai, C. Hough, R.D. Fields, R.M. Caudle, P.M. Blumberg, M.J. Iadarola, Ligand-induced dynamic membrane changes and cell deletion conferred by vanilloid receptor 1, J. Biol. Chem. 276 (2001) 11021–11030.
[26] W. Blum, L. Pecze, E. Felley-Bosco, J. Worthmuller-Rodriguez, L. Wu, B. Vrugt, M. de Perrot, B. Schwaller, Establishment of immortalized murine mesothelial cells and a novel mesothelioma cell line, In Vitro Cell. Dev. Biol. Anim. (2015).
[27] L. Pecze, B. Schwaller, Characterization and modeling of Ca(2+) oscillations in mouse primary mesothelial cells, Biochim. Biophys. Acta 1854 (2015) 632–645.
[28] R.D.C. Team, R: A Language and Environment for Statistical Computing, the R Foundation for Statistical Computing, 2011 (Place Published).
[29] Z. Olah, K. Josvay, L. Pecze, T. Letoha, N. Babai, D. Budai, F. Otvos, S. Szalma, C. Vizler, Anti-calmodulins and tricyclic adjuvants in pain therapy block the TRPV1 channel, PLoS One 2 (2007) e545.
[30] E. Scemes, C. Giaume, Astrocyte calcium waves: what they are and what they do, Glia 54 (2006) 716–725.
[31] Y.J. Sung, Z. Sung, C.L. Ho, M.T. Lin, J.S. Wang, S.C. Yang, Y.J. Chen, C.H. Lin, Intercellular calcium waves mediate preferential cell growth toward the wound edge in polarized hepatic cells, Exp. Cell Res. 287 (2003) 209–218.
[32] L. Pecze, W. Blum, B. Schwaller, Routes of Ca2+ Shuttling during Ca2+ Oscillations; Focus on the Role of Mitochondrial Ca2+ Handling and Cytosolic Ca2+ Buffers, J. Biol. Chem. (2015).
[33] G. Hajnoczky, L.D. Robb-Gaspers, M.B. Seitz, A.P. Thomas, Decoding of cytosolic calcium oscillations in the mitochondria, Cell 82 (1995) 415–424.
[34] V. Gogvadze, S. Orrenius, B. Zhivotovsky, Mitochondria in cancer cells: what is so special about them? Trends Cell Biol. 18 (2008) 165–173.
[35] L. Pecze, W. Blum, B. Schwaller, Mechanism of capsaicin receptor TRPV1-mediated toxicity in pain-sensing neurons focusing on the effects of Na(+)/Ca(2+) fluxes and the Ca(2+)-binding protein calretinin, Biochim. Biophys. Acta 1833 (2013) 1680–1691.
[36] H. Ouadid-Ahidouch, I. Dhennin-Duthille, M. Gautier, H. Sevestre, A. Ahidouch, TRP calcium channel and breast cancer: expression, role and correlation with clinical parameters, Bull. Cancer 99 (2012) 655–664.
[37] L. Zhao, X. Zhang, H. Kuang, J. Wu, Y. Guo, L. Ma, Effect of TRPV1 channel on the proliferation and apoptosis in asthmatic rat airway smooth muscle cells, Exp. Lung Res. 39 (2013) 283–294.
[42] M.J. Caterina, M.A. Schumacher, M. Tominaga, T.A. Rosen, J.D. Levine, D. Julius, The capsaicin receptor: a heat-activated ion channel in the pain pathway, Nature 389 (1997) 816–824.
[43] J.N. Wood, J. Winter, I.F. James, H.P. Rang, J. Yeats, S. Bevan, Capsaicin-induced ion fluxes in dorsal root ganglion cells in culture, J. Neurosci. 8 (1988) 3208–3220.
[44] A. Macho, M.A. Calzado, J. Munoz-Blanco, C. Gomez-Diaz, C. Gajate, F. Mollinedo, P. Navas, E. Munoz, Selective induction of apoptosis by capsaicin in transformed cells: the role of reactive oxygen species and calcium, Cell Death Differ. 6 (1999) 155–165.
[45] T. Rohacs, B. Thyagarajan, V. Lukacs, Phospholipase C mediated modulation of TRPV1 channels, Mol. Neurobiol. 37 (2008) 153–163.
[46] X. Zhang, S. Mak, L. Li, A. Parra, B. Denlinger, C. Belmonte, P.A. McNaughton, Direct inhibition of the cold-activated TRPM8 ion channel by Galphaq, Nat. Cell Biol. 14 (2012) 851–858.
[47] V. Lehen'kyi, N. Prevarskaya, in: M.X. Zhu (Ed.), Study of TRP Channels in Cancer Cells, TRP Channels, 2011 (Place Published).
[48] I. Dhennin-Duthille, M. Masson, E. Damiens, C. Fillebeen, G. Spik, J. Mazurier, Lactoferrin upregulates the expression of CD4 antigen through the stimulation of the mitogen-activated protein kinase in the human lymphoblastic T Jurkat cell line, J. Cell. Biochem. 79 (2000) 583–593.
[49] R.E. Dolmetsch, K. Xu, R.S. Lewis, Calcium oscillations increase the efficiency and specificity of gene expression, Nature 392 (1998) 933–936.
[50] S. Kupzig, S.A. Walker, P.J. Cullen, The frequencies of calcium oscillations are optimized for efficient calcium-mediated activation of Ras and the ERK/MAPK cascade, Proc. Natl. Acad. Sci. U. S. A. 102 (2005) 7577–7582.
[51] K. Campbell, K. Swann, Ca2+ oscillations stimulate an ATP increase during fertilization of mouse eggs, Dev. Biol. 298 (2006) 225–233.
[52] N.A. Venier, A.J. Colquhoun, N.E. Fleshner, L.H. Klotz, V. Venkateswara, Lycopene enhances the anti-proliferative and pro-apoptotic effects of capsaicin in prostate cancer in vitro, J. Cancer Ther. Res. 1 (2012).
[53] S. Malagarie-Cazenave, N. Olea-Herrero, D. Vara, I. Diaz-Laviada, Capsaicin, a component of red peppers, induces expression of androgen receptor via PI3K and MAPK pathways in prostate LNCaP cells, FEBS Lett. 583 (2009) 141–147.
[54] B.A. Saykali, M. El-Sibai, Invadopodia, regulation, and assembly in cancer cell invasion, Cell Commun. Adhes. 21 (2014) 207–212.
[55] G.P. Pidgeon, J. Lysaght, S. Krishnamoorthy, J.V. Reynolds, K. O'Byrne, D. Nie, K.V. Honn, Lipoxygenase metabolism: roles in tumor progression and survival, Cancer Metastasis Rev. 26 (2007) 503–524.
[56] R. Natarajan, J. Nadler, Role of lipoxygenases in breast cancer, Front. Biosci. 3 (1998) E81–E88.
[57] S.A. Spindler, F.H. Sarkar, W.A. Sakr, M.L. Blackburn, A.W. Bull, M. LaGattuta, R.G. Reddy, Production of 13-hydroxyoctadecadienoic acid (13-HODE) by prostate tumors and cell lines, Biochem. Biophys. Res. Commun. 239 (1997) 775–781.
[58] K. Kaszas, J.M. Keller, C. Coddou, S.K. Mishra, M.A. Hoon, S. Stojilkovic, K.A. Jacobson, M.J. Iadarola, Small molecule positive allosteric modulation of TRPV1 activation by vanilloids and acidic pH, J. Pharmacol. Exp. Ther. 340 (2012) 152–160.
[59] Y. Kato, S. Ozawa, C. Miyamoto, Y. Maehata, A. Suzuki, T. Maeda, Y. Baba, Acidic extracellular microenvironment and cancer, Cancer Cell Int. 13 (2013) 89.
[60] A.B. Gerry, D.S. Leake, Effect of low extracellular pH on NF-kappaB activation in macrophages, Atherosclerosis 233 (2014) 537–544.
[61] L.Y., C. Wu, J. Chen, K.H. Gotlinger, E. Ramu, J.R. Falck, M.L. Schwartzman, CYP4F isoform expression and 20-HETE synthesis in prostate cancer cells are regulated by androgen and contribute to growth, Proceedings of the 103rd Annual Meeting of the American Association for Cancer Research; 2012 Mar 31-Apr 4, Cancer Res, 72(8 Suppl), AACR, Chicago, IL. Philadelphia (PA), 2012 (Abstract nr LB-160. doi: 1538–7445.AM2012-LB-160 2012).
[62] H. Wen, J. Ostman, K.J. Bubb, C. Panayiotou, J.V. Priestley, M.D. Baker, A. Ahluwalia, 20-Hydroxyeicosatetraenoic acid (20-HETE) is a novel activator of transient receptor potential vanilloid 1 (TRPV1) channel, J. Biol. Chem. 287 (2012) 13868–13876.
[63] X. Gao, D.J. Grignon, T. Chbihi, A. Zacharek, Y.Q. Chen, W. Sakr, A.T. Porter, J.D. Crissman, J.E. Pontes, I.J. Powell, et al., Elevated 12-lipoxygenase mRNA expression correlates with advanced stage and poor differentiation of human prostate cancer, Urology 46 (1995) 227–237.
[64] D. Nie, G.G. Hillman, T. Geddes, K. Tang, C. Pierson, D.J. Grignon, K.V. Honn, Platelet-type 12-lipoxygenase in a human prostate carcinoma stimulates angiogenesis and tumor growth, Cancer Res. 58 (1998) 4047–4051.
[65] C. Xie, D.H. Wang, Inhibition of renin release by arachidonic acid metabolites, 12(s)-HPETE and 12-HETE: role of TRPV1 channels, Endocrinology 152 (2011) 3811–3819.